Supplementary Material

Robust longitudinal spin-Seebeck effect in Bi-YIG thin films

Gene Siegel, Megan Campbell Prestgard, Shiang Teng and Ashutosh Tiwari*

Nanostructured Materials Research Laboratory
Department of Materials Science and Engineering
University of Utah

* E-mail: tiwari@eng.utah.edu

SSE of platinum films grown on phase-separated Bi-YIG

In order to understand the possible cause of the ferromagnet-like MR characteristics in Pt films in Huang et al.'s[15] study, we prepared Bi-YIG films under un-optimized conditions (deposition temperature > 800 ^oC at $5x10^{-5}$ mbar of oxygen pressure and without any post annealing). XPS characterization of these films revealed a clear precipitation of Fe on the surface (see Fig. S1(a)). Pt films were deposited on these phase-separated Bi-YIG films and MR and SSE measurements were performed. MR data has been shown in Fig. 2(c) in the main-text while the SSE data is shown in Fig. S1(b).

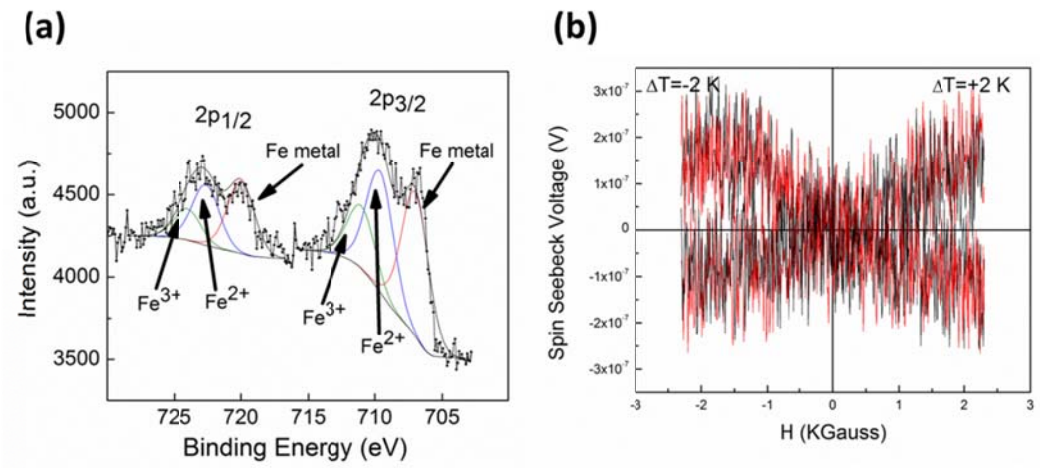

Fig. S1: a) XPS showing Fe-precipitation on the sample surface. b) Longitudinal SSE data showing much smaller SSE signal (and no hysteresis) compared to optimized Bi-YIG films.

Here it can be noticed that the XPS spectra of the Bi:YIG film grown under regular conditions and under unoptimized conditions show a significant difference in signal to noise ratio. The above difference is mainly because of the fact that these measurements were performed in different runs.

Recent discovery of spin Hall magnetoresistance

The absence of MR in our Pt films (10 nm thick) grown on optimized Bi-YIG film was contrary to the recently discovered phenomenon of spin Hall magnetoresistance (SMR). We conjecture that the extremely rough surfaces in our films may be responsible for the absence of detectable SMR signal. Our speculations are consistent with the theory of SMR which tells that the SMR depends very sensitively on the spin mixing conductance. So the variations in the interface quality could lead to significant changes and suppression in the MR magnitude. It has also been predicted that the SMR has a characteristic length scale; so we performed MR measurements on a thinner film (~4 nm thick) too. Results of those measurements are shown in Fig. S2.

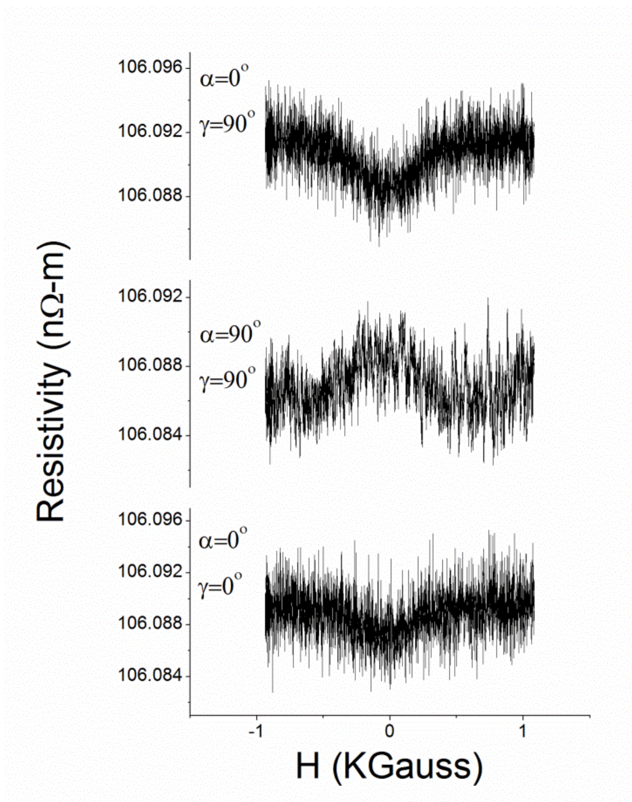

Fig. S2: Magnetoresistance of a ~4 nm thick Pt film (deposited under the optimized condition) for different orientations of the magnetic field and current. "α" and "γ" are the angles defined in the Fig. 4(c) of ref-21. Presence of a very slight SMR-like signal was noticed but because of the extremely small thickness and rough surface, noise level in the signal was very high. This forbade us to make any conclusion about the presence or absence of SMR in the film. More work, preferably with smother films is required to further explore this aspect.

Anglular dependence of longitudinal SSE data

The angular dependence of the SSE signal exhibited a cosine dependence as expected for the SSE phenomenon.

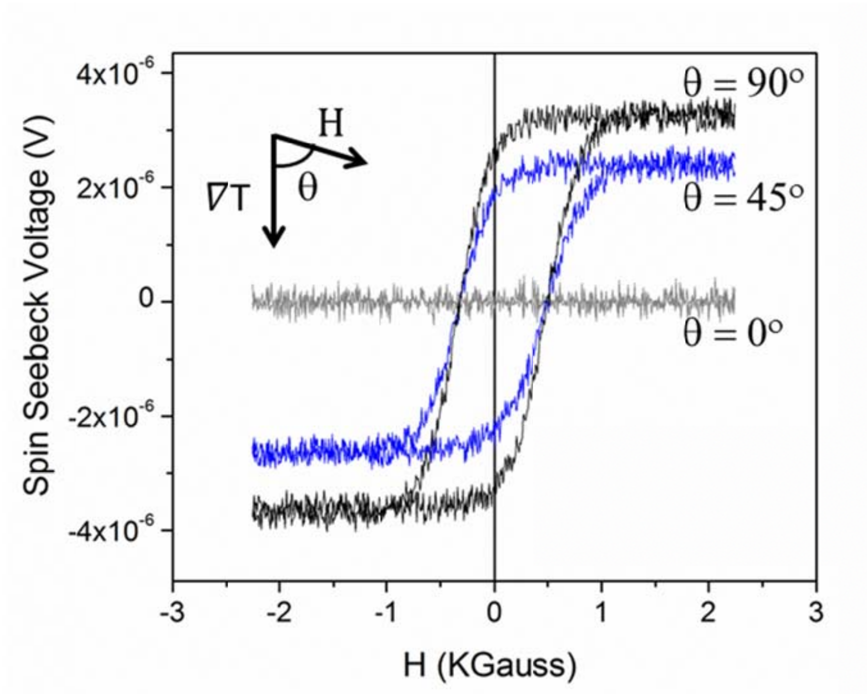

Fig. S3:.Longitudinal SSE voltage as a function of the applied magnetic field for ΔT=+2 K at 300K for three different values of 'θ'. Maximum value of the SSE voltage was observed when the temperature gradient and the magnetic field were perpendicular to each other while an almost negligible voltage was observed when those were parallel to each other. These results are in full agreement with the predictions of the SSE theory.

SSE measurements on transverse devices

To compare the transport characteristics of spin waves in the longitudinal devices with those in the transverse devices, we prepared the latter and performed temperature dependent SSE measurements. Fig. S4(a) shows a schematic of the transverse device. The Bi-YIG film was grown on a 10 mm x 5 mm GGG (111) substrate using the same protocol as the films for the longitudinal devices. Over this film, 10 nm thick platinum wires (100 um wide) were deposited by e-beam evaporation using a shadow mask. A magnetic field of 2K-Gauss and a temperature gradient of 2 K was applied between the two ends of the device. The voltage developed across the platinum strips was measured as a function of the base temperature of the device over the temperature range 20-300K. Fig. S4(b) shows the transverse SSE hysteresis loops at different temperatures. Fig. S4(c) shows the variation of Vss as a function of temperature. In contrast to longitudinal devices [Fig. S4(d) and Fig. S4(e)], SSE of transverse device showed an increase at low temperatures. These results are similar to those reported by Adachi et al.[17] and point towards the potential role played by the phonon drag process in the transverse geometry.

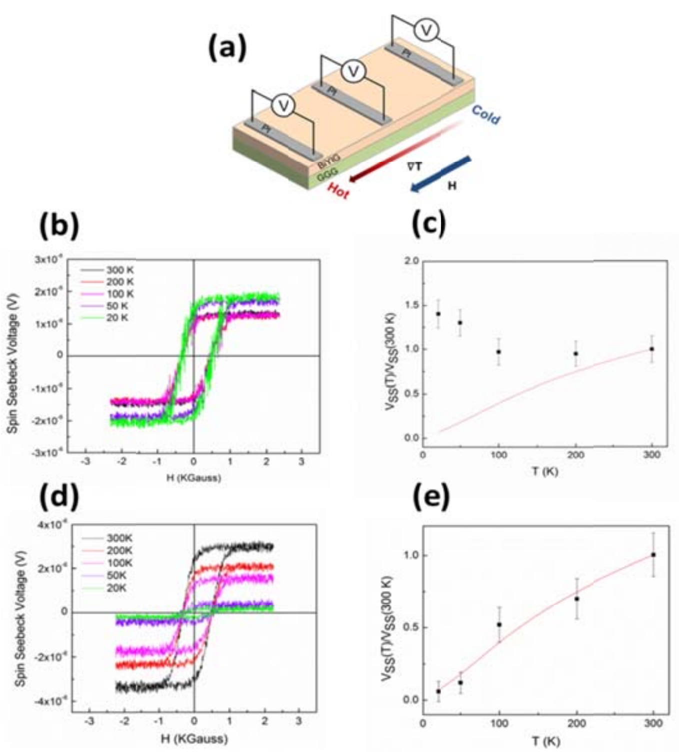

Fig. S4: a) Schematic of transverse SSE device. b) transverse SSE hysteresis loops at different temperatures for a temperature gradient of +2 K. c) Plot of transverse SSE data vs. temperature. d) Longitudinal SSE hysteresis loops at different temperatures for a temperature gradient of +2 K. c) Plot of longitudinal SSE data vs. temperature.

Theoretical calculation of SSE voltage using magnon transport theory

The normalized spin Seebeck voltage Vss(T)/Vss(300 K) (shown in Fig.4(b)) was calculated using the magnon transport theory.[26] For this, first the value of the magnon mediated spin current $|\boldsymbol{I_S}|$, injected into the platinum layer, was estimated using the relation:[17,26,27]

$$|\boldsymbol{I_S}| = \Delta T\left(\frac{P}{\alpha}\right)\int_0^{T_M/T} ds\,\frac{(T/T_M)s^2}{4\sinh^2\left(\frac{s}{2}\right)} = \Delta T\left(\frac{P}{\alpha}\right)I'_s$$

where α is the Gilbert damping constant, P is a nearly temperature independent coefficient calculated by Adachi et al.[17] , T_M is the magnon temperature and ΔT is the temperature difference (=2 K in the present case).

To calculate $I_S{}'$, we solved the integral:

$$I'_S = \int_0^{T_M/T} ds\,\frac{(T/T_M)s^2}{4\sinh^2\left(\frac{s}{2}\right)}$$

For this, the integral was expanded using Wolfram|Alpha software package** to:

$$\frac{T}{4T_M}\left\{2s\left[s + 4log(1-e^{-s}) + s\left(-coth\left(\frac{S}{2}\right)\right)\right] - 8Li_2(e^{-s})\right\} + constant\Big|_0^{T_M/T}$$

Where the $Li_2(e^{-s})$ is a poly logarithmic function with a general form of $Li_n(z)$ where

$$Li_n(z) = \sum_{k=1}^{\infty}\frac{z^k}{k^n}$$

$$Li_2(e^{-s}) = \sum_{k=1}^{\infty}\frac{e^{-sk}}{k^2}$$

Therefore, $I_S{}'$can be expressed as

$$I_S{}' = \frac{T}{4T_M}\left\{2\frac{T_M}{T}\left[\frac{T_M}{T} + 4log\left(1-e^{-\frac{T_M}{T}}\right) + \frac{T_M}{T}\left(-coth\left(\frac{T_M}{2T}\right)\right)\right] - 8\sum_{k=1}^{\infty}\frac{e^{-\frac{T_M}{T}k}}{k^2} + 16\right\}$$

Using the above expression, the values of $I_S{}'$ were estimated at different temperatures and then these values were used to estimate the value of the injected spin current $|\boldsymbol{I_S}|$. Once the values of $|\boldsymbol{I_S}|$ at different temperatures were known, those along with the experimentally measured values of the platinum resistivity (ρ) were substituted in equation-1 (of the main text) to estimate the value of Vss(T)/Vss(300 K). θ_{SH}, α and P were taken to be temperature independent[17] and magnetic field was perpendicular to the applied temperature gradient. The value of T_M for Bi-YIG was taken as 560K.

** http://www.wolframalpha.com/

Effect of enhanced coercivity on the SSE

As discussed in the main text of the paper, an enhanced coercivity observed in our films can hold the magnetization stable along a direction where the SSE effect is maximal. This is a very import aspect, because it provides a way to design devices which remain functional even in the absence of an external magnetic field. However, this also means that thermally induced magnetic excitations will be of relatively lower amplitude and therefore the corresponding heat-to-spin conversion efficiency can be smaller.

Furthermore, the non-square shaped *M vs H* hysteresis loops exhibited by the Bi-YIG films are indicative of only a partial, non-simultaneous magnetization reversal i.e. the sample magnetization at zero applied magnetic field is not fully saturated. So, in order to achieve the maximum SSE voltage, a relatively large field needs to be applied to saturate the Bi-YIG magnetization. As can be seen in Fig.3, at room temperature the SSE voltage for zero applied magnetic field was about 80% of the maximum SSE voltage.